Case Studies in Construction Materials 16 (2022) e01112

Contents lists available at ScienceDirect

Case Studies in Construction Materials

journal homepage: www.elsevier.com/locate/cscm

Chloride induced corrosion of steel reinforcement in alkali activated slag concretes: A critical review

Tran Huyen Vu [a], Liet Chi Dang [b], Gyeongo Kang [b,*], Vute Sirivivatnanon [a]

[a] School of Civil and Environmental Engineering, University of Technology Sydney, Broadway, NSW, Australia
[b] Department of Civil Engineering, Gwangju University, 277 Hyodeok-ro, Nam-gu, Gwangju 61743, South Korea

ARTICLE INFO

Keywords:
Chloride induced corrosion
Chloride binding
Chloride threshold
Steel reinforcement
Geopolymer
Alkali activated materials

ABSTRACT

Alkali activated materials (AAMs) have been recognised as potential alternatives to Portland cement concretes in specific applications in the construction industry due to their environmental benefits such as substantially reduced CO_2 emissions and utilisation of industrial wastes. While many studies reported the superior performance of AAM concretes over Portland cement concretes in protecting steel from corrosion, some other studies indicated an opposite view. Hence, there is a need for further research on the long-term corrosion studies of AAM concretes in the laboratory as well as in the field. Among many important areas of investigation is the resistance of AAMs to chloride induced corrosion of steel reinforcement which is not well understood. In this paper, the above aspect is reviewed including chloride ingress, chloride binding and chloride induced corrosion rate of steel reinforcement in AAMs. Chloride ingress in AAMs involves both open and closed pore systems. Chloride binding in AAMs is predominantly physical and not chemical. The chloride threshold levels initiating steel corrosion in AAMs are significantly different in comparison to Portland cement concretes.

1. Introduction

Sustainable construction has become increasingly important to achieve lasting structures and to decrease the environmental impact of the construction industry. An important step to achieve sustainability in construction is using environmentally friendly construction materials [112,113]. Industrial by-products and other wastes such as fly ash and slag have been used as supplementary cementitious materials for cost reduction and improvements in durability [1–3]. Alkali activated materials (AAMs), a new binder compared to Portland cement, is manufactured using predominantly fly ash and slag, and selected alkali activators [4]. AAMs do not require high temperature kilns for manufacture. Thus, they do not require significant levels of fuel energy as ordinary Portland cement (OPC) does. The production of OPC, a traditional binder, not only consumes a large quantity of natural resources and energy but also releases a significant amount of greenhouse gases into the atmosphere [5–7]. In Australia, in order to reduce greenhouse gas emissions, considerable efforts have been made by cement manufacturers through significant investments in new kiln technology, alternative fuels, raw materials, and energy efficiency [8]. Despite these efforts, greenhouse gas emissions in cement production pose a major challenge. On the other hand, it is generally accepted that production of AAMs has much lower CO_2 emissions [9–11]. Further, AAMs can be designed to have superior durability properties such as high resistance to alkali-silica reaction, freeze-thaw, acid attack and sulphate attack [10,12–15,109], by changing the type of precursor, the type and concentration of activator, and curing regime

* Corresponding author.
E-mail address: gokang@gwangju.ac.kr (G. Kang).

https://doi.org/10.1016/j.cscm.2022.e01112
Received 27 January 2022; Received in revised form 20 April 2022; Accepted 26 April 2022
Available online 6 May 2022

[16–19]. Therefore, attempts have been made to replace Portland cement based concrete with AAM concrete in certain applications such as precast products [3,20]. However, the application of AAM in structure applications is still limited until now because available information on service history and durability performance of alkali activated concrete products is not sufficient to receive the public acceptance as a construction material [110]. Also, the use of sodium hydroxide and mainly sodium silicate, used in the production of activated alkali materials, produces emission of greenhouse gases pollutants [111]. However, compared with the emission of greenhouse gases pollutants by the OPC production, activated alkali materials are still a greener choice.

AAMs are formed by the reactions between aluminosilicate precursors, or source materials and alkaline activators [5,7]. Aluminosilicate precursors are classified into three main groups:

Low calcium such as low calcium fly ash and meta-kaolin;
High calcium such as slag and
A blend of these two types such as a blend of fly ash and slag.

AAMs produced from a low calcium aluminosilicate precursor is deemed as geopolymer [5,7]. Those produced from a blend of low calcium precursors and high calcium ones (for example, a blend of fly ash and slag) are also considered as geopolymer [21]. A blend of fly ash and slag is increasingly being investigated due to the benefits that can be derived from the presence of both types (see Fig. 1) in the binder system [22].

Corrosion of steel reinforcement is a major durability issue of the reinforced concrete structures using Portland cement concrete in many parts of the world [23,24]. One of the main causes of steel corrosion in reinforced concrete structures is the ingress of chloride ions into concrete [24]. Thus, to assess whether AAMs are viable alternatives to replace Portland cement in reinforced concrete structures, the resistance of AAMs to chloride induced corrosion needs thorough investigation. Until now, published results on chloride induced corrosion in AAM concretes are limited and ambiguous. This paper provides the current state-of-the-art of chloride induced corrosion in AAM concretes, including chloride penetration, chloride binding and corrosion rate.

2. Reduction in CO_2 emissions from the production of AAM concretes

The environmental benefits of AAMs are still being debated [25,26]. However, a comparison of CO_2 emissions of a 40 grade fly ash/slag based powder form of geopolymer concrete and same grade OPC concrete, clearly reveals the environmental benefit of considerably reduced emission of geopolymer concrete. To be more specific, a grade 40 OPC mix revealed 354 kg of CO_2 emission equivalent [27] against 145 kg of CO_2 emission equivalent for fly ash/slag based powder form of geopolymer concrete mix (calculated), currently being investigated. The details of such calculations for a geopolymer concrete mix, with a 28-day compressive strength of 46 MPa, are presented in Table 1.

In Table 1, sodium silicate was used in solid form, which released 1.14 kg CO_2/kg [28]. However, if sodium silicate was used in liquid form, the amount of CO_2 released would be 0.424 kg CO_2/kg which was much lower than that of the solid form. This result was similar to previously published results [30], supporting the fact that CO_2 emissions are considerably lower for AAMs.

3. Corrosion of steel reinforcement in AAM concrete

In reinforced concrete structures with OPC concrete, the corrosion of steel reinforcement commences when passive films on the surface of steel are partly or completely broken down. These films are the dense iron oxide layers comprising crystalline layers of Fe_3O_4 with outer layers of γ-Fe_2O_3 [31]. Fe_3O_4 and Fe_2O_3 are formed on the steel surface at the high alkalinity of the pore solution, as shown in Fig. 2. These passive films on the steel surface vary in thickness (from 1 to 10 nm) and composition, depending on the availability of

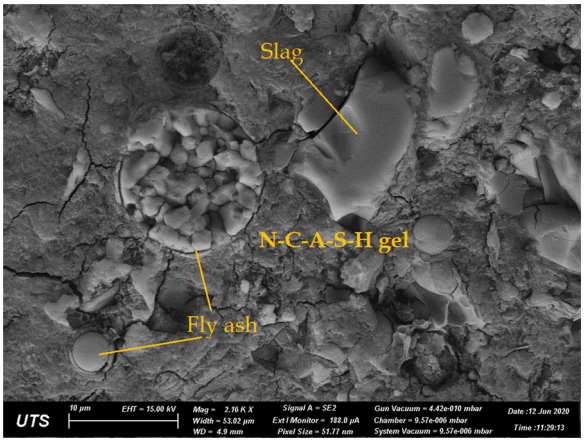

Fig. 1. Microstructure of geopolymer based on fly ash and slag.

Table 1
CO_2 emissions per m^3 of geopolymer concrete.

Activities			Quantity of CO_2 emissions (kg)	Reference
Placement			9	[27]
Transport			9	
Curing (at ambient temperature)			< 1	
Batching			3	
Materials	kg/m^3	kg	CO_2 emissions (kg)	Reference
Aggregate	1223.6	0.0408	49.9	[26]
Sand	779.6	0.0139	10.9	
Fly ash	180.7	0.0270	4.9	
Slag	115.6	0.1430	16.6	
Sodium silicate (solid form)	28.9	1.1400	33.0	[28]
Sodium carbonate	28.9	0.2300	6.7	[29]
Admixture	7.3		< 1	
Total CO_2 emissions (kg)			145	

oxygen, water, alkalinity and type of ions in the pore solution [32,33]. Passive films are 'self-healing' in nature but the presence of anions such as chlorides can locally destroy the films and initiate corrosion. These layers cannot stop corrosion but can prevent iron from dissolving and reduce the corrosion rate to an insignificant level [24]. The reduction in corrosion rate could be of the order of magnitude of 4–6 [34]. The steel corrosion rate in this region is about 0.1 μm/year [35].

Fig. 3 illustrates the passivation of steel in terms of corrosion rate. As the potential of steel varies from negative to positive at a certain potential, the metal forms a protective film on the surface. Above this potential, it remains passive and the reactivity is decreased. If the potential is increased still further, the current density again increases in the trans-passive region. Conversely, in the case of reinforcement corrosion, the potential decreases in the negative region and once a "threshold potential" is reached, steel will start to corrode below this potential.

There are two main causes that can break down the passive oxide film on the steel surface. One is carbonation which reduces the pH of concrete, and another is the presence of chloride ions [38,39]. Chloride attack is dominant in environments where the concrete surface comes into contact with chloride ions such as marine and coastal areas. When chloride ions at the surface of the steel build up to a certain amount, the threshold value, with the presence of water and oxygen, the protective film is locally destroyed [40,41]. In this process, chloride ions play a key role of catalysts, stimulating further corrosion reactions, as illustrated in Fig. 4.

Steel corrosion leads to products (rust) that have larger volumes (6 times more) than the volume of original steel that they replaced, as shown in Fig. 5. Formation of rust results in a reduction in the cross-sectional area of steel reinforcement and a significant loss of bond between the steel and the surrounding concrete [42].

Nonetheless, the corrosion of steel in AAM concretes is not understood well yet. Limited information is available in this regard, particularly, corrosion of steel in AAMs in the presence of chloride ions. It is important to understand the interaction of steel with AAM matrix around it. Recent research has clearly shown that the nature and stability of the passive film change when the steel bar was embedded in AAM concrete. Because of the high alkalinity and high sulphide content of AAS, there were differences in the redox and chemical characteristics of the pore solutions of concrete made of alkali-activated slag (AAS) and OPC [44,45].

Sulphides present at the steel-AAM concrete interface due to chemical reactions offer some protection against corrosion of steel reinforcement [46]. Corrosion behaviour of steel embedded in alkali-activated slag mortars exposed to an alkaline solution, alkaline

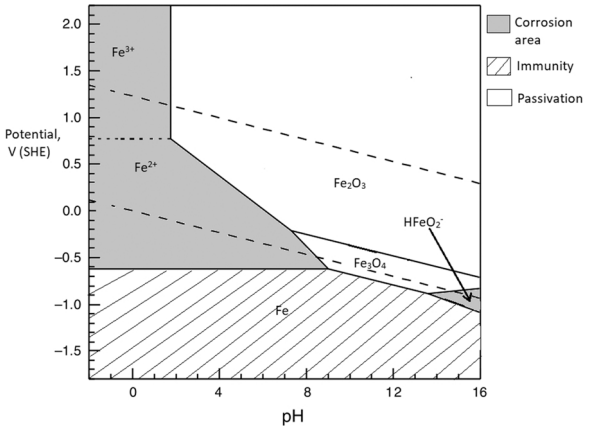

Fig. 2. Pourbaix diagram for iron in a chloride-free aqueous solution at 25 °C (modified from Pourbaix [36]).

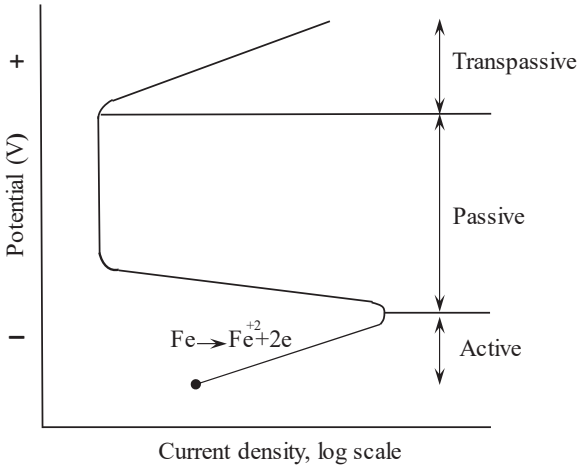

Fig. 3. Passive region in steel corrosion [37].

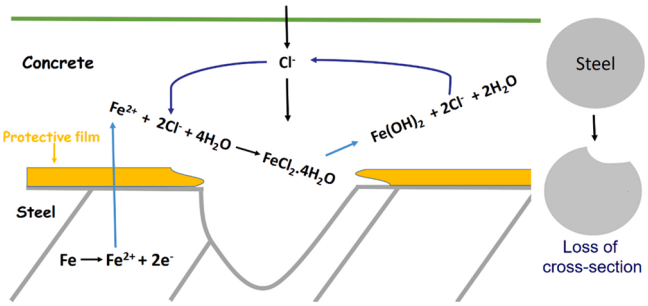

Fig. 4. Role of chloride ions as catalysts to steel corrosion.

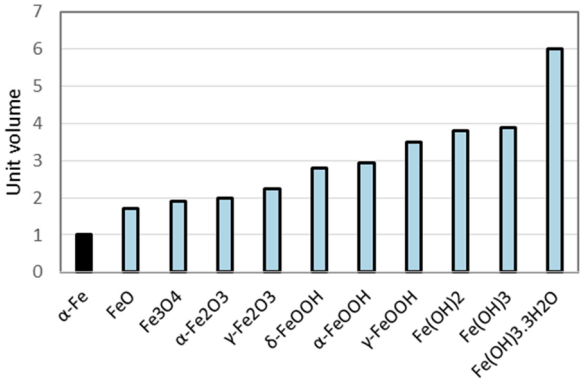

Fig. 5. Volume of corrosion products in relation to the volume of original steel (modified from Poursaee [43]).

chloride-rich solution and water under standard laboratory conditions, was investigated using electrochemical techniques. The steel embedded in alkali-activated slag mortars presented very negative electric potentials and high apparent corrosion current values. The presence of sulphide reduced the electric potential, and the oxidation of the reduced sulphur-containing chemicals within the cement itself gave an electrochemical signal. In electrochemical tests for reinforced concrete durability, this would have been interpreted as a signal due to steel corrosion processes. However, the actually observed resistance to chloride-induced corrosion in this investigation was very high, as measured by extraction and characterisation of the steel at the end of a 9-month exposure period.

The onset of chloride-induced pitting on the steel surface (in simulated alkali-activated slag pore solution) depends on both the concentration of sulphide and the time of exposure, due to the alteration of passive film chemistry in the presence of a strong reductant, which is beneficial in restricting corrosion if the sulphide concentration is sufficiently high [45].

The impact of the Al–Si precursors on the exchanges between the steel and the AAM matrix was studied on geopolymer solutions with various concentrations of alkali and Si/Al ratios [47]. For this investigation, Fourier-transform infrared (FTIR) spectroscopy-specular reflectance, X-ray photoelectron spectroscopy (XPS) and Auger spectroscopy (AES) were used. At the interface, a transition zone was identified in which the Si/Al ratio differed from the bulk matrix. At the interface, the Si/Al ratio was less than 1, which implied that at the interface there was more Al than Si, and that the Fe species on the steel substrate preferentially interact with the Al species in the solution. XPS and FTIR results also showed that the formation of the Al–O–Fe bond could be due to the chemical reactions between iron-based substances and polymer gel. The gel has reacted with the oxide layer on steel, forming this transition zone.

Chloride diffusion and chloride binding are two important aspects in assessing the resistance of geopolymers to chloride induced corrosion of steel embedded in it. Chloride binding will be discussed in detail in Section 5.2. The formation of a passive layer on the steel reinforcement embedded in fly ash geopolymer mortars was observed after approximately two weeks of hardening at the laboratory temperature [48]. However, alternative heat-treatment at 80 °C for several hours led to the formation of the passive layer immediately.

The information presented and discussed above clearly indicates the differences between OPC concrete and geopolymer concretes. The key areas where differences exist and need further investigation are the nature and thickness of passive film formation, corrosion potentials at corrosion initiation, the volume of corrosion products, transition zone and interactions between concrete products and steel surface and nature of pit formation and corrosion rate. In addition, the chloride ion movement and diffusion, chloride binding capacity and threshold chloride concentration which are key parameters for chloride induced corrosion of steel in geopolymer concrete are discussed in detail below.

4. Chloride induced corrosion of steel reinforcement in AAMs

A comparison between corrosion of steel reinforcement in AAM and OPC concretes reported contradicting results (see Table 2).

4.1. Fly ash geopolymer concrete

Some studies reported that the fly ash geopolymer mortars passivated steel reinforcement as effectively as Portland cement mortars [49,50]. Others reported that the fly ash geopolymer concrete showed superior resistance to chloride attack, with a longer time to corrosion on-set, compared to OPC concrete [51,52]. Further, Monticelli et al. [54] studied the corrosion behaviour of steel in fly ash geopolymer mortars, cured under various conditions (at room temperature) and exposed to chlorides. The corrosion process was monitored by polarisation resistance and corrosion potential measurements. A lower chloride content, when compared with OPC mortars with the same cover, was measured at the steel-concrete interface in the geopolymer mortar. The reinforcement in geopolymer also exhibited significantly higher corrosion resistance than that in cement [60]; however, the stability properties of the passivation film of reinforcement in cement is better than that of reinforcement in geopolymer.

In contrast, studies on the severity of steel corrosion in fly ash geopolymer concrete culverts, over 6 years and 10 years of exposure in a saline lake environment, reported a different trend [55,56]. Visual observation, SEM/EDX analysis of the steel/concrete interface and the result of higher chloride penetration were combined to reach a conclusion that higher corrosion activity of the steel bar was present in fly ash geopolymer concrete [55,56], compared with that of OPC concrete culvert of a similar strength grade. The reason for these differences could be attributed to the different methods used to measure corrosion rate. Instead of the above methods, many

Table 2
Corrosion of steel reinforcement in AAM and OPC concretes.

Type of AAM concrete	Passivated steel reinforcement, compared with OPC concrete	Method	References
Fly ash geopolymer	As effectively as	Corrosion potential Polarisation resistance	[49,50]
	Better	SEM Chloride diffusion Corrosion potential Visual examination	[51]
		Current intensity due to specimen cracking Mass loss measurements	[52]
		SEM Corrosion potential Polarisation resistance	[53,54]
	Worse	XRD SEM/EDX Visual examination	[55,56]
Fly ash/slag geopolymer	Better	Chloride diffusion Corrosion potential	[57]
Alkali activated slag	Better	Chloride diffusion Mass loss measurement Electrical resistance during chloride ponding test	[58]
	Worse	Corrosion potential	[59]

researchers used direct measurements on the steel bars such as the corrosion potential (E_{corr}) measurements and the polarisation resistance (R_p) in various studies [49–52]. These methods were not used for the above culverts.

4.2. Fly ash/slag geopolymer concrete

Most studies on the chloride induced corrosion of steel reinforcement in fly ash/slag blended geopolymer concretes showed that such concretes (with suitable ratios of fly ash to slag) have excellent resistance against corrosion of steel reinforcement. This is probably due to the fact that the appropriate combination of fly ash and slag as source materials for producing geopolymer has an advantage over using either fly ash or slag alone. It is ascertained that the main reaction product of alkaline activation of slag is CSH gel [61–63], while that of fly ash is geopolymer gel or N-A-S-H or K-A-S-H gel. The coexistence of these two gels can make the resultant matrix denser because the formation of C-S-H and N-A-S-H gels may help bridge the gaps between the different hydrated phases and unreacted particles [64]. Also, C-S-H gel serves as a micro-aggregate, which can improve the strength of geopolymer concrete [64]. It is generally believed that OPC concrete with lower porosity makes it difficult for the chloride ions to reach the steel surface. Thus, fly ash/slag geopolymer concrete of a similar grade is expected to have better durability due to the presence of a closed pore structure. Recently, the effectiveness of 50% fly ash/50% slag geopolymer in improving the microstructure of resulting geopolymers was confirmed using SEM by Saha and Rajasekaran [65].

In another study, the corrosion of the reinforcement in 50% fly ash/50% slag geopolymer concrete and OPC concrete was compared [57]. Fly ash/slag geopolymer concrete had compressive strengths of about 50 MPa at the age of 28 days and the OPC concrete was a 40 grade mix with a w/c ratio of 0.46 and cement content of 400 kg (geopolymer mix also had a binder content of 400 kg and w/c ratio of 0.43). Also, 2% NaCl by mass of binder was added in geopolymer and OPC mixes to assess the corrosion behaviour of steel reinforcement in contaminated concretes. All reinforced samples (95 mm × 95 mm× 300 mm), with a thickness of concrete cover 40 mm, were then partially immersed in water. From 0–150 days, the half-cell potential of steel embedded in geopolymer concrete was in the range of − 500 to − 550 mV, more negative than that of steel embedded in OPC concrete (from −350 to −400 mV). This indicated a higher corrosion degree of embedded steel in geopolymer concrete. However, results obtained by visual inspection showed a different trend. The steel embedded in OPC concrete showed a high level of corrosion after 150 days, while the steel embedded in geopolymer concrete did not show any pitting corrosion products. It was concluded that half-cell potential results seemed to misrepresent the corrosion state of steel reinforcement in contaminated fly ash/slag geopolymer concrete.

4.3. Alkali activated slag concrete

The evolution of the corrosion potential and current density of reinforced alkali activated slag (AAS) and OPC concretes were observed by Chaparro, Ruiz & Gosmez [59]. These two types of concrete were prepared with liquid/solid of 0.4. Reinforced AAS and OPC concrete cylinders (76.2 mm diameter and 76.2 mm length), with cover thickness 35 mm, after cured in a climatic chamber for 28 days at 90% relative humidity for AAS specimens and at 100% RH for OPC specimens, were immersed in 3.5% NaCl solution over 12 months. In the first 3 months, results of the corrosion potential and current density showed low levels of corrosion for AAS and OPC concretes. From 3 months to 6 months, a similar likelihood of corrosion for AAS and OPC concretes was observed. For the following 6 months, the probability of corrosion was higher in AAS concrete. However, there were no results about compressive strength and pore characteristic of AAS and OPC concretes in this work. If these two important parameters of AAS and OPC concretes were simultaneously investigated with the corrosion potential of steel reinforcement embedded in such concretes, it would be more persuasive.

In 2009, VicRoads in Australia undertook the construction of the reinforced alkali activated slag concrete retaining walls at the west abutment of Swan Street Bridge, Melbourne, so as to further understand the practical potential of alkali activated slag concrete [66]. In order to monitor the long term performance of alkali activated slag concrete and the corrosion of steel reinforcement in these retaining walls, three MnO_2 half-cell reference electrodes were embedded in the concrete at the time of construction of the walls. The half-cell

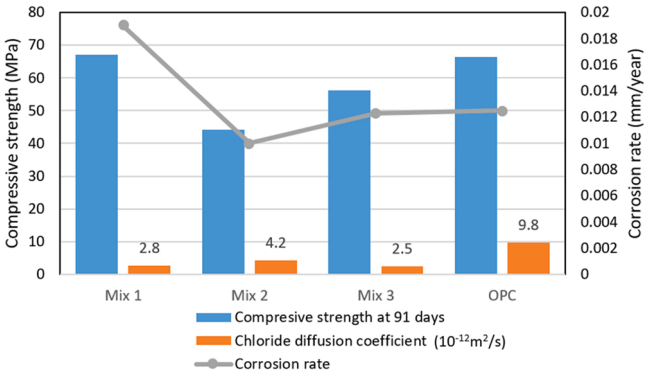

Fig. 6. Compressive strength at 91 days, chloride diffusion coefficient and corrosion rate of the AAS (Mix 1, Mix 2 and Mix 3) and OPC concretes [58].

potentials between reinforcing steel and reference electrode were measured at the different locations using a multimeter. Following that, there were the extractions of concrete cores for strength testing and microstructural examination. Alkali activated slag (AAS) concrete was prepared with a binder content of 400 kg/m^3, solid activator (sodium meta-silicate anhydrous) 5–10% of binder and water/binder (w/b) ratio of 0.52–0.57. This AAS concrete met the 40 MPa strength requirement of VicRoads Specification (Section 610), but its porosity measured using VPV (19.3%) did not meet the requirement of 16%. The half-cell potential measurements of steel embedded in this AAS concrete retaining walls were stable at approximately − 350 mV (CSE) after 2 years, implying less likelihood of corrosion [66].

In a study by Ma et al. [58], the corrosion rates of the steel bars measured in some AAS concretes were comparable to that in the OPC concrete with identical binder contents and w/b ratios. In all mixes, the binder content was constant at 400 kg/m^3 and the w/b ratio was 0.47. The non-steady state chloride diffusion coefficient (D_{nssd}) of the AAS concrete, measured by NT BUILD 443 (immersed for 3 months in a 2.82 M NaCl solution), was much lower than that of OPC concrete. A possible reason for the lower chloride diffusion coefficient of AAS concretes was probably because of the better pore structure, the stronger interaction between hydration products and the improved chloride binding for the AAS concretes. This trend was clearly evident despite the lower initial compressive strength of several AAS concrete mixes (see Fig. 6).

5. Penetration of chloride ions in AAM concrete

5.1. Limitations and improvements in the methods of testing chloride penetration

For testing penetration of chloride ions in AAMs, the most popular methods are rapid chloride permeability test (RCPT) specified in ASTM C1202 [67], NordTest NT Build 443 (similar to ASTM C1556) [68], and NordTest NT Build 492 [69]. RCPT measures chloride ion migration or electrical conductivity of concrete. This method only provides charge passed due to the movement of ions and does not measure the depth of chloride penetration. In this technique, a voltage of 60 V is applied across the ends of slices of a concrete cylinder in 6 h. One face is in contact with sodium chloride solution, and the other is in contact with sodium hydroxide solution, as shown in Fig. 7. This test method, however, has some disadvantages. Apart from structural damages caused by the higher applied voltage and the associated temperature increase, this test is considered as an unsuitable indicator of the chloride resistance of the AAM concretes[70,71]. In other words, high performing AAM concrete with better resistance to chloride ions and a higher alkali concentration in pore solution allowed more charge to pass (indicating higher chloride permeability) than those of moderately performing AAM concretes [72]. Hence, RCPT gave unreliable results for AAM concretes. However, a modified version of this test method is useful for testing chloride penetration in AAM concretes in the field application because this is a rapid and portable test. Recently, a modified RCPT test was proposed by using 10 V, instead of 60 V. By using this modified test, a good correlation was observed between the charge passed and the chloride diffusion coefficient measured by ASTM C1556 or NT Build 443 [73]. The prospect of adopting a modified RCPT test to establish a practical method for testing chloride penetration in AAM concrete serves as a stimulus for future research.

On the other hand, NT Build 492 is a non-steady state migration test using an external electrical potential to force the chloride ions from outside to migrate into the specimen. Thus, this test can avoid some of the drawbacks of the ASTM C 1202 test because it uses a lower applied potential (typically 30 V) and longer test duration (in 24 h) [74]. Meanwhile, NT Build 443 is a type of ponding test, where one face of a cylindrical specimen is exposed to a 2.8 M NaCl solution for at least 35 days and then the chloride profile is measured. According to RILEM Technical Committee 247-DTA Report [72], both NT Build 492 and NT Build 443 showed acceptable outcomes within laboratory reproducibility, but the results between the different laboratories were scattered. Hence, the tests for chloride penetration in AAM concretes have not been finalised yet. Numerous research activities to solve this problem, however, are in progress now.

5.2. Chloride binding in AAM concrete

When chloride ions from the external environment penetrate concretes, a proportion of them is bound by the hydration products.

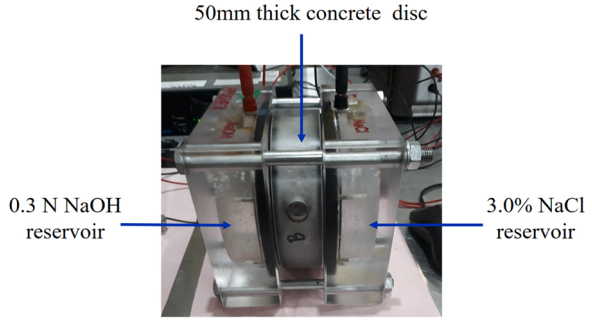

Fig. 7. Rapid chloride permeability test.

This process of chloride binding can reduce the free chloride concentration in the solution, and hence it impacts the chloride threshold and decreases the likelihood of steel corrosion. However, bound chlorides can be transformed into free chlorides, under some conditions where the chemical equilibrium between bound and free chlorides are disturbed [75,76], so bound chlorides also pose some risk to steel corrosion and must be controlled.

In Portland cement binder, chloride ions can be bound chemically by the formation of Friedel's salt, which is created by the reaction between chlorides and cement compounds such as C_3A and C_4AF [77]. There is no C_3A or C_4AF in the alkali activated binder, and hence the mechanism of how chlorides are bound in the AAM matrix, if that happens at all, may be different to that in Portland cement and needs to be investigated. In fact, powder X-ray diffraction (XRD) was used to find out about this aspect of AAM. Alkali activated slag mortars were prepared with the addition of high content of sodium chloride in the mixing water. XRD results did not show formations of any new crystalline phases even at the highest level of NaCl addition (13% by weight of slag), and no significant peaks were seen in the region $8 \pm 13^{\circ}$ 2θ which is expected for Friedel's salt [78]. As for alkali activated fly ash mortars (or fly ash geopolymer mortars), even after immersing in NaCl solution for 2 years, there was no formation of new crystalline phases such as the ettringite or Friedel's salt [79]. There might be other chloride bearing substances in the AAM concrete. It is a fact that the activation process of fly ash produces the main reaction product with a structure similar to zeolite precursor, a three-dimensional framework [80,81]. Also, the secondary reaction product of this process is zeolite [10,82], as shown in Fig. 8. It is well known that zeolite is an absorbent of several ions and molecules. For example, it has been used as an absorbent material for seawater desalination [83,84]. It is primarily because zeolites have a micro porous structure with a highly regular structure of pores and chambers, also large surface area that can accommodate a wide variety of ions. Hence, the ability of a geopolymer concrete to bind chloride ions might be associated with the absorption properties of reaction products of the activation process. This conclusion was confirmed by the results obtained in a recent study by Lee & Lee [85]. There were no differences observed in XRD results between the alkali activated fly ash/slag pastes of un-immersed and immersed (in 10% NaCl solution for 90 days) specimens. However, the bound chloride contents in the pastes, immersed in 10% NaCl solution, was in the range of 68–94% (by weight of total chlorides). Additionally, the bound chloride content increased with the increase of fly ash content. Hence, it could be concluded that chloride ions can be absorbed by zeolite precursors and zeolites in AAM mortars or concretes.

In Portland cement paste, chlorides can be present in the pore solution or physically held to the surface of hydration products C-S-H gel [86]. The alkaline activation process of blast furnace slag also produces C-S-H (calcium silicate hydrate) gel, as the main reaction product, similar to the gel obtained during Portland cement hydration [10]. Therefore, the chloride ions in AAMs with slag can also be physically bound, similar to that in the Portland cement binder. Further, alkali activated slag cements were found to contain hydrotalcite-group phases as a hydration product, and this provides surface adsorption in the diffuse layer that can further restrict the ingress of chloride [87].

The average chloride binding capacity of the geopolymer concretes is low in comparison to Portland cement concretes. There does not seem to be a chemical reaction between geopolymer binders and chloride ions. According to recent research, it was concluded that the binding capacity of geopolymers is mainly due to adsorption or encapsulation of the chlorides within the geopolymer pore network [88]. Chloride bearing characteristics of alkali activated slag was also investigated at different salinity level [89]. Chloride bearing solid phase includes Cl-hydrocalumite and Cl-hydrotalcite [89]. However, this area requires further investigation.

Further, most of the factors affecting the chloride binding in the Portland cement based binder involve their influences on the solubility of Friedel's salt [90]. Accordingly, the parameters changing the chloride binding in the AAMs may be different to those in the Portland cement systems. For example, increasing the NaOH concentration (from 8 M to 18 M) in the fly ash activated concretes resulted in a rise in the chloride binding capacity (from 14% to 30%, respectively) and improved compressive strength (from 23.4 to 30.3 MPa), also a denser microstructure [91]. The bound chloride percentage, by weight of the total chloride penetration, of fly ash alkali activated concretes increased from 51% to 63% when the CaO content in the fly ash increased from 0.64% to 4.80% [53]. Calcined layered double hydroxide (CLDH) due to its ion-exchange properties can increase in chloride binding capacity of alkali

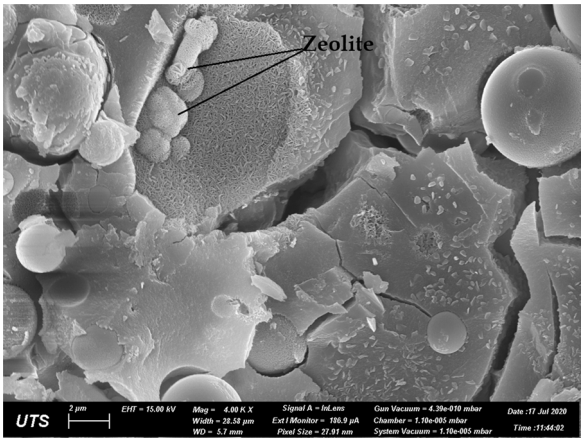

Fig. 8. Zeolite crystal in geopolymer system.

activated slag [87]. Curing regimes can significantly affect the activation of geopolymerisation process, resulting in dense and less porous geopolymer matrix, and thus increasing the physical adsorption and chemical binding of chloride ions on the gel surface [92]. However, very few studies have been carried out on this important aspect until now.

5.3. Correlation between the penetration of chloride ions and pore characteristics

In many situations basically, compressive strength has been considered as an indirect parameter to predict the resistance of concrete to chloride penetration [93]. However, for AAM concrete, the chloride penetration did not correlate well with the compressive strength [57,73,94]. In reality, the penetration of chloride ions from an external environment into cementitious materials is a complex phenomenon, involving multiple mechanisms such as diffusion, permeation and capillary absorption. Diffusion is assumed to be the principal transport of chloride ion movement in concretes where the pores are saturated and there is a chloride concentration gradient [95]. Chloride diffusion is governed by Fick's First Law, similar to other diffusion processes. Besides, chloride diffusion is more easily measured in the laboratory, compared with the other mechanisms. Permeation is associated with a high hydrostatic pressure applied on one face of the concrete, which seldom happens. Capillary absorption is driven by moisture gradient, in which chloride ions are brought into the pores of concrete via capillary suction. However, this mechanism just takes place at a shallow cover region [95]. All these mechanisms involve the transport of chloride ions (0.368 nm diameter) through macropores of a few mm in size, micropores and continuous capillary pores down to 10 nm size. Below about 10 nm size pores (called gel pores in OPC concrete) the transport of chloride ions is unlikely.

For AAM concrete, however, the size of pores formed and the pore size distribution can be different to OPC concrete because of different chemical gels that are formed and hence changing the tortuosity. Studying the porosity, pore characteristics (e.g. tortuosity) and pore size distribution of AAM concretes is, thus, vital for understanding the transport of chloride ions, rather than just concentrating on mechanical properties such as compressive strength. In order to measure porosity in AAM concretes, the volume of permeable voids (VPV) (as per ASTM C642 or AS 1012.21) is commonly used because this method is quite easily performed in the laboratory. Based on the permeable pore amount of the concrete, the ability of the concrete to withstand an aggressive environment can be evaluated. When applying the above type of tests to AAMs, the process of drying samples might harm the microstructure of such materials. Therefore, the drying process of samples should be given due consideration and carried out carefully. There are some recommendations about the selection of drying methods. Ismail & Bernal [96] proposed that if the material contains a significant amount of chemically bound water (such as alkali-activated slag), drying should be achieved by the acetone method. If the material has a small quantity of chemically bound water (such as binders based on fly ash or metakaolin), then drying should be achieved by either vacuum or acetone methods [96]. Drying samples at 60 °C in lieu of 100 °C until reaching constant weight could be useful to avoid the excessive desiccation of the binding phases that is induced by thermal drying in alkali activated slag binders [71].

6. Factors affecting chloride induced corrosion of steel reinforcement in AAM concrete

The main factors affecting the corrosion resistance of steed rebar embedded in geopolymer concrete against the attack of chlorides are identified as chemistry and quantity of raw materials, the nature of activators and the concentration of sulphur species in the pore solution. These factors are discussed in detail below:

6.1. Chemistry and quantity of raw materials

The presence of calcium in source materials was believed to be extremely important to reduce the alkali mobility or alkali loss which decreases the pore solution pH, and so causes depassivation of protective film on embedded steel [97]. However, in terms of the microstructure of the geopolymer concrete, it might not be appropriate. It is because geopolymer concrete that is produced from fly ash with high calcium content showed higher porosity than that produced with fly ash having low calcium content [98]. The substitution of 20–40% fly ash by slag in the fly ash/slag geopolymer concrete mix at the constant liquid/solid of 0.7 does not change the porosity significantly but reduces the sizes of pores and also increases the tortuosity, resulting in a reduced porosity and an increased tortuosity [99]. As a result of this, the chloride penetration rate is decreased.

The variation of slag content in the mix design of fly ash/slag geopolymer concrete affected the chloride-binding capacity and the resistance to chloride penetration in a different way. Increasing the slag content up to 50% in the mixes resulted in an increase of C-(A)-S-H gel, leading to the denser geopolymer concretes. Therefore, the chloride penetration depth was greatly decreased [85]. However, they pointed out that the chloride-binding capacity increased with the amount of N-A-S-H gels and when the slag content was increased, the chloride binding capacity was decreased.

6.2. The nature of activators

The alkali concentration (Na_2O %) and silica modulus (Ms, the molar ratio of SiO_2/Na_2O) of the alkaline activating solution were found to control the non-steady state diffusion coefficient D_{nssd} of the AAS concrete [58]. Increasing Na_2O content from 4% to 8% led to a decrease in D_{nssd}. The lowest D_{nssd} was obtained with AAM concrete using an activator with Ms of 1.50. This study also suggested that activator with Ms of 1.5 and Na_2O of 6% was the optimum content to achieve the lowest D_{nssd} and corrosion rate. In another study on the durability of AAS mortar [100], the optimum content of sodium was 10%, which yielded a higher level of strength and lower porosity. When fly ash geopolymer concrete was prepared from an alkaline activator having a high NaOH concentration, the quantity

of free and total chloride ions penetration was decreased. This led to a decrease of the chloride diffusion coefficient and steel corrosion in this geopolymer concrete, after 3 years of exposure in a marine environment [91]. The type of alkali cation was found to considerably affect the chloride binding of metakaolin/fly ash geopolymers, in which sodium activator results in stronger chloride binding capacity and better resistance to chloride penetration, compared to potassium-based activator [101]. It is because Na has a higher capacity of promoting the dissolution of solid aluminosilicates, geopolymerization, and zeolitization, despite the fact that KOH activator has a higher level of alkalinity at the same OH^- concentration, due to the large ionic size of K cation. This led to the comparatively high amount of N-A-S-H gel and zeolite products formed in Na-geopolymer than that of K-A-S-H in K-geopolymer, resulting in the enhanced Na-geopolymer with a higher chloride binding capacity than its K-counterpart.

6.3. The concentration of sulphur species in the pore solution

The corrosion rate of steel rebar in AAS concretes was observed to decrease with the increase of the concentration of sulphur contained species in the pore solution [102]. The sulphide concentration investigated in this study was up to 0.1 M; however, the percentage of the corrosion rate was not specially mentioned in the study. This observation was also recorded in another study by Ma et al. [58]. This phenomenon in AAM concrete is quite similar to that in Portland cement [103]. It was explained that the presence of sulphur species in the pore solution of concrete such as HS^-, S^{2-} and SO_3^{2-} provided a reducing internal environment which could decrease the dissolved oxygen in the pore solution, and hence considerably reduce the redox potential, or the reduction potential, of the pore solution. This would protect the embedded steel from its oxidation, and thus reduce the probability of corrosion of the steel. Therefore, source materials which are rich in sulphide would be preferable to the production of AAM concrete. The critical role of HS^- in defining mild steel passivation chemistry was also investigated in a study by Mundra & Provis [104]. The film formed on the steel surface in alkaline-sulphide solutions contains $Fe(OH)_2$ and Fe–S complexes, and the critical chloride concentration to induce corrosion increases at high sulphide concentration. However, some other studies reported that when the sulphur content was high, the formation of FeS film on the steel surface was preferential instead of the oxide film. This weakened the passive layer on the steel surface [103,105–108].

7. Conclusions and recommendations for future research

Based on the findings presented above, the following conclusions have been drawn:

- Some researchers compared the performance of different strength grades of AAM and OPC concrete in their corrosion studies. The basis of this comparison is not valid. The performance of AAM concretes should be compared with that of OPC or blended cement based concretes that have similar strength grades, in relation to chloride induced corrosion to make the comparison valid.
- Fly ash/slag blended geopolymer concrete with appropriate mix design could serve as an effective alternative for OPC concrete in reinforced concrete structures. However, on the aspect of chloride induced corrosion, information is lacking, and more work is needed.
- Chloride ion movement and diffusion in AAM concretes require long-term diffusion tests or accelerated chloride penetration tests at low voltages. High voltage tests applicable to OPC concretes cannot be applied to AAMs. This area needs further research.
- Chloride binding mechanisms in AAM concretes are predominantly physical unlike in OPC concretes where they are both chemical and physical.
- The investigation of chloride binding in term of the mechanism of how chloride ions are bound into AAM matrices, the dependence of chloride binding on mix design of AAM concretes is another open avenue for researchers.
- The chloride threshold levels to initiate corrosion in AAM concretes appear to be more than that of OPC concretes. Chloride threshold levels in AAMs, however, need to be established.
- Factors affecting chloride threshold levels to initiate corrosion in AAM concretes is still unclear. Further investigations are needed to carry out in this area.
- Interface transition zone (ITZ) and passive film formation on steel surface in AAM concrete and its breakdown mechanisms need further research.
- Half- cell potential results to initiate corrosion in AAM concretes are lower than those in OPC concretes. Reliable threshold values for different AAMs need to be established.

Declaration of Competing Interest

The authors declare that they have no known competing financial interests or personal relationships that could have appeared to influence the work reported in this paper.

Acknowledgements

This work was supported by the National Research Foundation of Korea (NRF) grant funded by the Korea government (MSIT) (No. 2021R1C1C2004070) and the research funds from Gwangju University in 2022. I would like to express my gratitude to Dr. Nadarajah Gowripalan and Associate Professor Pre De Silva for kindly supporting the first author to complete this study.

References

[1] A. Fernández-Jiménez, N. Cristelo, T. Miranda, Á. Palomo, Sustainable alkali activated materials: precursor and activator derived from industrial wastes, J. Clean. Prod. 162 (2017) 1200–1209, https://doi.org/10.1016/j.jclepro.2017.06.151.
[2] H.A. Abdel-Gawwad, S.A. Mohamed, M.S. Mohammed, Recycling of slag and lead-bearing sludge in the cleaner production of alkali activated cement with high performance and microbial resistivity, J. Clean. Prod. 220 (2019) 568–580, https://doi.org/10.1016/j.jclepro.2019.02.144.
[3] M. Nawaz, A. Heitor, M. Sivakumar, Geopolymers in construction - recent developments, Constr. Build. Mater. 260 (2020), 120472, https://doi.org/10.1016/j.conbuildmat.2020.120472.
[4] P. Awoyera, A. Adesina, A critical review on application of alkali activated slag as a sustainable composite binder, Case Stud. Constr. Mater. 11 (2019), e00268, https://doi.org/10.1016/j.cscm.2019.e00268.
[5] P. Duxson, A. Fernández-Jiménez, J.L. Provis, G.C. Lukey, A. Palomo, J.S.J. van Deventer, Geopolymer technology: the current state of the art, J. Mater. Sci. 42 (2007) 2917–2933, https://doi.org/10.1007/s10853-006-0637-z.
[6] J.L. Provis, Geopolymers and other alkali activated materials: why, how, and what? Mater. Struct. 47 (2014) 11–25, https://doi.org/10.1617/s11527-013-0211-5.
[7] J.L. Provis, S.A. Bernal, Geopolymers and related alkali-activated materials, Annu. Rev. Mater. Res. 44 (2014) 3–29, https://doi.org/10.1146/annurev-matsci-070813-113515.
[8] Australia Cement Industry Federation, Industry Report 2017, (2017).
[9] W.S. Li Wang, Honghu Tang Ning Sun, A review on comprehensive utilization of red mud, Minerals 9 (2019), https://doi.org/10.3390/min9060362.
[10] A. Palomo, P. Krivenko, I. Garcia-Lodeiro, E. Kavalerova, O. Maltseva, A. Fernández-Jiménez, A review on alkaline activation: new analytical perspectives, Mater. Constr. 64 (2014), e022.
[11] J. Davidovits, Geopolymer chemistry and sustainable development. The poly (sialate) terminology: a very useful and simple model for the promotion and understanding of green-chemistry, 2005 Geopolymer Conference (2005) 9–15.
[12] B. Panda, S.C. Paul, L.J. Hui, Y.W.D. Tay, M.J. Tan, Additive manufacturing of geopolymer for sustainable built environment, J. Clean. Prod. 167 (2017) 281–288, https://doi.org/10.1016/j.jclepro.2017.08.165.
[13] M. Amran, A. Al-Fakih, S.H. Chu, R. Fediuk, S. Haruna, A. Azevedo, N. Vatin, Long-term durability properties of geopolymer concrete: an in-depth review, Case Stud. Constr. Mater. 15 (2021), e00661, https://doi.org/10.1016/j.cscm.2021.e00661.
[14] J. Davidovits, Properties of geopolymer cements, First International Conference on Alkaline Cement and Concretes, Kiev (1994) 131–149.
[15] F. Pacheco-torgal, Z. Abdollahnejad, A.F. Camões, M. Jamshidi, Y. Ding, Durability of alkali-activated binders: a clear advantage over Portland cement or an unproven issue ? Constr. Build. Mater. 30 (2012) 400–405, https://doi.org/10.1016/j.conbuildmat.2011.12.017.
[16] Draft- background infomation, n.d.
[17] Z. Podolsky, J. Liu, H. Dinh, J.H. Doh, M. Guerrieri, S. Fragomeni, State of the art on the application of waste materials in geopolymer concrete, Case Stud. Constr. Mater. 15 (2021), e00637, https://doi.org/10.1016/j.cscm.2021.e00637.
[18] P. Chindaprasirt, P. Jitsangiam, W. Chalee, U. Rattanasak, Case study of the application of pervious fly ash geopolymer concrete for neutralization of acidic wastewater, Case Stud. Constr. Mater. 15 (2021), e00770, https://doi.org/10.1016/j.cscm.2021.e00770.
[19] S.K. John, Y. Nadir, K. Girija, Effect of source materials, additives on the mechanical properties and durability of fly ash and fly ash-slag geopolymer mortar: a review, Constr. Build. Mater. 280 (2021), 122443, https://doi.org/10.1016/j.conbuildmat.2021.122443.
[20] A.L. Almutairi, B.A. Tayeh, A. Adesina, H.F. Isleem, A.M. Zeyad, Potential applications of geopolymer concrete in construction: a review, Case Stud. Constr. Mater. 15 (2021), e00733, https://doi.org/10.1016/j.cscm.2021.e00733.
[21] J. Davidovits, The manufacture of geopolymer cements, in: Geopolymer Chemistry and Applications. Institut Géopolymère, Saint-Quentin France, 2015, pp. 537–568.
[22] B.A. Tayeh, A.M. Zeyad, I.S. Agwa, M. Amin, Effect of elevated temperatures on mechanical properties of lightweight geopolymer concrete, Case Stud. Constr. Mater. 15 (2021), e00673, https://doi.org/10.1016/j.cscm.2021.e00673.
[23] M. El-Reedy, Introduction, in: Steel-Reinforced Concrete Structures: Assessment and Repair of Corrosions, Taylor & Francis Group, The United States of America, 2008, pp. 1–3.
[24] Portland Cement Association, Types and Causes of Concrete Deterioration, 2002.
[25] J. Davidovits, False Values on CO2 Emission for Geopolymer Cement/Concrete published in Scientific Papers, Technical Paper #24, Geopolymer Institute Library, 2015.
[26] F. Collins, Inclusion of carbonation during the life cycle of built and recycled concrete: influence on their carbon footprint, Int. J. Life Cycle Assess. 15 (2010) 549–556, https://doi.org/10.1007/s11367-010-0191-4.
[27] L.K. Turner, F.G. Collins, Carbon dioxide equivalent (CO_2-e) emissions: a comparison between geopolymer and OPC cement concrete, Constr. Build. Mater. 43 (2013) 125–130, https://doi.org/10.1016/j.conbuildmat.2013.01.023.
[28] M. Fawer, M. Concannon, W. Rieber, Life cycle inventories for the production of sodium silicates, Int. J. Life Cycle Assess. 4 (1999) 207–212, https://doi.org/10.1007/BF02979498.
[29] IPCC Guidelines for National Greenhouse Gas Inventories, Chapter 2. Industrial processes, (1996). ⟨https://doi.org/10.1002/masy.200450406⟩.
[30] B.C. McLellan, R.P. Williams, J. Lay, A. Van Riessen, G.D. Corder, Costs and carbon emissions for geopolymer pastes in comparison to ordinary portland cement, J. Clean. Prod. 19 (2011) 1080–1090, https://doi.org/10.1016/j.jclepro.2011.02.010.
[31] P.M. Chess, Corrosion in reinforced concrete structures, in: P.M. Chess, J. Broomfield (Eds.), Cathodic Protection of Steel in Concrete and Masonry, Taylor & Francis Group, 2014, pp. 1–16.
[32] M. Cohen, The formation and properties of passive films on iron, Can. J. Chem. 37 (2006) 286–291, https://doi.org/10.1139/v59-037.
[33] V. Maurice, P. Marcus, Current developments of nanoscale insight into corrosion protection by passive oxide films, Curr. Opin. Solid State Mater. Sci. 22 (2018) 156–167, https://doi.org/10.1016/j.cossms.2018.05.004.
[34] J.O.M. Bockris, A.K.N. Reddy, Chapter 8. Electrodics, in: Modern Electrochemistry, vol. II, Plenum Press, New York, 1970, pp. 845–908.
[35] C.M. Hansson, The corrosion of steel and zirconium in anaerobic concrete, MRS Online Proc. Libr. Arch. 50 (1985).
[36] M. Pourbaix, Atlas of Electrochemical Equilibria in Aqueous Solutions, National Association of Corrosion Engineers (NACE), Houston, Tex., 1974., National Association of Corrosion Engineers, 1974.
[37] G.P. Gu, J.J. Beaudoin, V.S. Ramachandran, Techniques for corrosion investigation in reinforced concrete, in: Handbook of Analytical Techniques in Concrete Science and Technology. Noyes Publications, New Jersey, 2001, pp. 441–504.
[38] C.L. Page, K.W.J. Treadaway, Aspects of the electrochemistry of steel in concrete, Nature 297 (1982) 109–115, https://doi.org/10.1038/297109a0.
[39] V.G. Papadakis, C.G. Vayenas, M.N. Fardis, A reaction engineering approach to the problem of concrete carbonation, AIChE J. 35 (1989) 1639–1650, https://doi.org/10.1002/aic.690351008.
[40] C.L. Page, Mechanism of corrosion protection in reinforced concrete marine structures, Nature 258 (1975) 514–515.
[41] K. Tuutti, Corrosion of steel in concrete, Stockholm, 1982.
[42] U. Angst, B. Elsener, C.K. Larsen, Ø. Vennesland, Chloride induced reinforcement corrosion: rate limiting step of early pitting corrosion, Electrochim. Acta 56 (2011) 5877–5889, https://doi.org/10.1016/j.electacta.2011.04.124.
[43] A. Poursaee, Corrosion of steel in concrete structures, in: Steel Corros (Ed.), Corrosion of Steel in Concrete Structures, Elsevier, 2016, pp. 19–34.
[44] S. Mundra, S.A. Bernal, M. Criado, P. Hlavá, G. Ebell, S. Reinemann, J.G. Gluth, J.L. Provis, Steel corrosion in reinforced alkali - activated materials (2017) 33–39.
[45] S. Mundra, S.A. Bernal, J.L. Provis, Corrosion initiation of steel reinforcement in simulated alkali-activated slag pore solutions, 1st International Conference of Construction Materials for Sustainable Future (2017).

[46] M. Criado, J.L. Provis, Alkali activated slag mortars provide high resistance to chloride-induced corrosion of steel, Front. Mater. 5 (2018) 1–15, https://doi.org/10.3389/fmats.2018.00034.
[47] S.L. Yong, D.W. Feng, G.C. Lukey, J.S.J. van Deventer, Chemical characterisation of the steel-geopolymeric gel interface, Colloids Surf. A Physicochem. Eng. Asp. 302 (2007) 411–423, https://doi.org/10.1016/j.colsurfa.2007.03.004.
[48] P. Hlaváček, S. Reinemann, G.J.G. Gluth, G. Ebell, H.-C. Kühne, J. Mietz, Steel reinforcement corrosion in alkali-activated fly ash mortars, in: International Conference on Alkali Activated Materials and Geopolymers: Versatile Materials Offering High Performance and Low Emissions, Curtin University, Australia, 2018, p. 300.
[49] D.M. Bastidas, A. Fernández-Jiménez, A. Palomo, J.A. González, A study on the passive state stability of steel embedded in activated fly ash mortars, Corros. Sci. 50 (2008) 1058–1065, https://doi.org/10.1016/j.corsci.2007.11.016.
[50] J.M. Miranda, A. Fernández-Jiménez, J.A. González, A. Palomo, Corrosion resistance in activated fly ash mortars, Cem. Concr. Res. 35 (2005) 1210–1217, https://doi.org/10.1016/j.cemconres.2004.07.030.
[51] K. Kupwade-Patil, E.N. Allouche, Examination of chloride-induced corrosion in reinforced geopolymer concretes, J. Mater. Civ. Eng. 25 (2013) 1465–1476, https://doi.org/10.1061/(ASCE)MT.1943-5533.0000672.
[52] D.V. Reddy, J.-B. Edouard, K. Sobhan, S.S. Rajpathak, Durability of reinforced fly ash-based geopolymer concrete in the marine environment, 36th Conference on Our World in Concrete & Structures, Singapore (2011) 14–26.
[53] C. Gunasekara, D. Law, S. Bhuiyan, S. Setunge, L. Ward, Chloride induced corrosion in different fly ash based geopolymer concretes, Constr. Build. Mater. 200 (2019) 502–513, https://doi.org/10.1016/j.conbuildmat.2018.12.168.
[54] C. Monticelli, M.E. Natali, A. Balbo, C. Chiavari, F. Zanotto, S. Manzi, M.C. Bignozzi, Corrosion behavior of steel in alkali-activated fly ash mortars in the light of their microstructural, mechanical and chemical characterization, Cem. Concr. Res. 80 (2016) 60–68, https://doi.org/10.1016/j.cemconres.2015.11.001.
[55] K. Pasupathy, D. Singh Cheema, J. Sanjayan, Durability performance of fly ash-based geopolymer concrete buried in saline environment for 10 years, Constr. Build. Mater. 281 (2021), 122596, https://doi.org/10.1016/j.conbuildmat.2021.122596.
[56] K. Pasupathy, M. Berndt, J. Sanjayan, P. Rajeev, D.S. Cheema, Durability of low - calcium fly ash based geopolymer concrete culvert in a saline environment, Cem. Concr. Res. 100 (2017) 297–310, https://doi.org/10.1016/j.cemconres.2017.07.010.
[57] C. Tennakoon, A. Shayan, J.G. Sanjayan, A. Xu, Chloride ingress and steel corrosion in geopolymer concrete based on long term tests, Mater. Des. 116 (2017) 287–299, https://doi.org/10.1016/j.matdes.2016.12.030.
[58] Q. Ma, S.V. Nanukuttan, P.A.M. Basheer, Y. Bai, Chloride transport and the resulting corrosion of steel bars in alkali activated slag concretes, Mater. Struct. 49 (2016) 3663–3677, https://doi.org/10.1617/s11527-015-0747-7.
[59] W.A. Chaparro, H.J.B. Ruiz, R.D.J.T. Gosmez, Corrosion of reinforcing bars embedded in alkali-activated slag concrete subjected to chloride attack, Mater. Res. 15 (2012) 57–62.
[60] L.F. Fan, W.L. Zhong, X.G. Zhang, Chloride-induced corrosion of reinforcement in simulated pore solution of geopolymer, Constr. Build. Mater. 291 (2021), 123385, https://doi.org/10.1016/j.conbuildmat.2021.123385.
[61] I.G. Richardson, A.R. Brough, G.W. Groves, C.M. Dobson, The characterization of hardened alkali-activated blast-furnace phase, Cem. Concr. Res. 24 (1994) 813–829.
[62] Z. Huanhai, W. Xuequan, X. Zhongzi, T. Mingshu, Kinetic study on hydration of alkali-activated slag, Cem. Concr. Res. 23 (1993) 1253–1258.
[63] A. Fernández-Jiménez, F. Puertas, I. Sobrados, J. Sanz, Structure of calcium silicate hydrates formed in alkaline-activated slag: influence of the type of alkaline activator, J. Am. Ceram. Soc. 86 (2003) 1389–1394.
[64] C.K. Yip, G.C. Lukey, J.S.J. van Deventer, The coexistence of geopolymeric gel and calcium silicate hydrate at the early stage of alkaline activation, Cem. Concr. Res. 35 (2005) 1688–1697, https://doi.org/10.1016/j.cemconres.2004.10.042.
[65] S. Saha, C. Rajasekaran, Enhancement of the properties of fly ash based geopolymer paste by incorporating ground granulated blast furnace slag, Constr. Build. Mater. 146 (2017) 615–620, https://doi.org/10.1016/j.conbuildmat.2017.04.139.
[66] A. Shayan, A. Xu, F. Andrews-phaedonos, Field performance of geopolymer concrete, used as a measure towards reducing carbon dioxide emission, in: Concrete Institutue of Australia Conference, Gold Coast, Queensland, Australia, 2013.
[67] American Society for Testing and Materials, Standard Test Method for Electrical Indication of Concrete's Ability to Resist Chloride (ASTM C1202-18), 2018.
[68] Nordtest, Concrete, hardened accelerated chloride penetration - NT Build 443, 1995.
[69] Nordtest, Chloride migration coefficient from non-steady-state migration experiments- NT Build 492, (1999) 1–8.
[70] D. Ravikumar, N. Neithalath, An electrical impedance investigation into the chloride ion transport resistance of alkali silicate powder activated slag concretes, Cem. Concr. Compos. 44 (2013) 58–68, https://doi.org/10.1016/j.cemconcomp.2013.06.002.
[71] I. Ismail, S.A. Bernal, J.L. Provis, R. San Nicolas, D.G. Brice, A.R. Kilcullen, S. Hamdan, J.S.J.Van Deventer, Influence of fly ash on the water and chloride permeability of alkali-activated slag mortars and concretes, Constr. Build. Mater. 48 (2013) 1187–1201, https://doi.org/10.1016/j.conbuildmat.2013.07.106.
[72] J.L. Provis, F. Winnefeld, Outcomes of the round robin tests of RILEM TC 247-DTA on the durability of alkali-activated concrete, MATEC Web Conf. 199 (2018).
[73] A. Noushini, A. Castel, Performance-based criteria to assess the suitability of geopolymer concrete in marine environments using modified ASTM C1202 and ASTM C1556 methods, Mater. Struct. Constr. 51 (2018) 1–16, https://doi.org/10.1617/s11527-018-1267-z.
[74] K. Vance, M. Aguayo, A. Dakhane, D. Ravikumar, J. Jain, N. Neithalath, Microstructural, mechanical, and durability related similarities in concretes based on OPC and alkali-activated slag binders, Int. J. Concr. Struct. Mater. 8 (2014) 289–299, https://doi.org/10.1007/s40069-014-0082-3.
[75] G.K. Glass, B. Reddy, N.R. Buenfeld, The participation of bound chloride in passive film breakdown on steel in concrete, Corros. Sci. 42 (2013) 2013–2021.
[76] B. Reddy, G.K. Glass, P.J. Lim, N.R. Buenfeld, On the corrosion risk presented by chloride bound in concrete, Cem. Concr. Compos. 24 (2002) 1–5.
[77] A. Delagrave, J. Marchand, J. Ollivier, S. Julien, K. Hazrati, Chloride binding capacity of various hydrated cement paste systems, Adv. Cem. Based Mater. 6 (1997) 28–35.
[78] A.R. Brough, M. Holloway, J. Sykes, A. Atkinson, Sodium silicate-based alkali-activated slag mortars Part II. The retarding effect of additions of sodium chloride or malic acid, Cem. Concr. Compos. 30 (2000) 1375–1380.
[79] F. Škvára, T. Jílek, L. Kopecký, Geopolymer materials based on fly ash, Ceramic 49 (2005) 195–204.
[80] A. Fernández-Jiménez, A. Palomo, I. Sobrados, J. Sanz, The role played by the reactive alumina content in the alkaline activation of fly ashes, Microporous Mesoporous Mater. 91 (2006) 111–119, https://doi.org/10.1016/j.micromeso.2005.11.015.
[81] A. Palomo, S. Alonso, A. Fernandez-jime, Alkaline activation of fly ashes: NMR study of the reaction products, J. Am. Ceram. Soc. 87 (2004) 1141–1145.
[82] A. Fernández-Jiménez, A. Palomo, M. Criado, Microstructure development of alkali-activated fly ash cement: a descriptive model, Cem. Concr. Res. 35 (2005) 1204–1209, https://doi.org/10.1016/j.cemconres.2004.08.021.
[83] T. Wajima, T. Shimizu, T. Yamato, Y. Ikegami, Removal of NaCl from seawater using natural zeolite, Toxicol. Environ. Chem. 92 (2010) 21–26, https://doi.org/10.1080/02772240902762958.
[84] E. Wibowo, M. Sutisna, R. Rokhmat, Khairurrijal Murniati, M. Abdullah, Utilization of natural zeolite as sorbent material for seawater desalination, Procedia Eng. 170 (2017) 8–13, https://doi.org/10.1016/j.proeng.2017.03.002.
[85] N.K. Lee, H.K. Lee, Influence of the slag content on the chloride and sulfuric acid resistances of alkali-activated fly ash/slag paste, Cem. Concr. Compos. 72 (2016) 168–179, https://doi.org/10.1016/j.cemconcomp.2016.06.004.
[86] J.J. Beaudoin, V.S. Ramachandran, R.F. Feldman, Interaction of chloride and C-S-H, Cem. Concr. Res. 20 (1990) 875–883.
[87] X. Ke, S.A. Bernal, J.L. Provis, Uptake of chloride and carbonate by Mg-Al and Ca-Al layered double hydroxides in simulated pore solutions of alkali-activated slag cement, Cem. Concr. Res. 100 (2017) 1–13, https://doi.org/10.1016/j.cemconres.2017.05.015.
[88] A. Noushini, A. Castel, J. Aldred, A. Rawal, Chloride diffusion resistance and chloride binding capacity of fly ash-based geopolymer concrete, Cem. Concr. Compos (2019), 103290, https://doi.org/10.1016/j.cemconcomp.2019.04.006.

[89] Y. Jun, T. Kim, J.H. Kim, Chloride-bearing characteristics of alkali-activated slag mixed with seawater: effect of different salinity levels, Cem. Concr. Compos. 112 (2020), 103680, https://doi.org/10.1016/j.cemconcomp.2020.103680.
[90] Q. Yuan, C. Shi, G. De Schutter, K. Audenaert, D. Deng, Chloride binding of cement-based materials subjected to external chloride environment - a review, Constr. Build. Mater. 23 (2009) 1–13, https://doi.org/10.1016/j.conbuildmat.2008.02.004.
[91] P. Chindaprasirt, W. Chalee, Effect of sodium hydroxide concentration on chloride penetration and steel corrosion of fly ash-based geopolymer concrete under marine site, Constr. Build. Mater. 63 (2014) 303–310, https://doi.org/10.1016/j.conbuildmat.2014.04.010.
[92] O.A. Mayhoub, A. Mohsen, Y.R. Alharbi, A.A. Abadel, A.O. Habib, M. Kohail, Effect of curing regimes on chloride binding capacity of geopolymer, Ain Shams Eng. J. (2021) 1–10, https://doi.org/10.1016/j.asej.2021.04.032.
[93] Cement Concrete & Aggregates Australia, Chloride Resistance of Concrete, 2009.
[94] A. Runci, M. Serdar, Chloride-induced corrosion of steel in Alkali-activated mortars based on different precursors, in: Materials, 13, 2020, pp. 1–17, https://doi.org/10.3390/ma13225244.
[95] R.D. Hooton, M.D.A. Thomas, K. Stanish, Prediction of chloride penetration in concrete, No. FHWA-RD-00-142, 2001, 2001.
[96] I. Ismail, S.A. Bernal, Microstructural changes in alkali activated fly ash / slag geopolymers with sulfate exposure (2013) 361–373. https://doi.org/10.1617/s11527-012-9906-2.
[97] R.R. Lloyd, J.L. Provis, J.S.J. Van Deventer, Pore solution composition and alkali diffusion in inorganic polymer cement, Cem. Concr. Res. 40 (2010) 1386–1392, https://doi.org/10.1016/j.cemconres.2010.04.008.
[98] M.S. Badar, K. Kupwade-patil, S.A. Bernal, J.L. Provis, E.N. Allouche, Corrosion of steel bars induced by accelerated carbonation in low and high calcium fly ash geopolymer concretes, Constr. Build. Mater. 61 (2014) 79–89, https://doi.org/10.1016/j.conbuildmat.2014.03.015.
[99] H. Zhu, Z. Zhang, Y. Zhu, L. Tian, Durability of alkali-activated fly ash concrete: chloride penetration in pastes and mortars, Constr. Build. Mater. 65 (2014) 51–59, https://doi.org/10.1016/j.conbuildmat.2014.04.110.
[100] M.T. Marvila, A.R.G. de Azevedo, L.B. de Oliveira, G. de Castro Xavier, C.M.F. Vieira, Mechanical, physical and durability properties of activated alkali cement based on blast furnace slag as a function of %Na2O, Case Stud. Constr. Mater. 15 (2021), e00723, https://doi.org/10.1016/j.cscm.2021.e00723.
[101] C. Fu, H. Ye, K. Zhu, D. Fang, J. Zhou, Alkali cation effects on chloride binding of alkali-activated fly ash and metakaolin geopolymers, Cem. Concr. Compos. 114 (2020), 103721, https://doi.org/10.1016/j.cemconcomp.2020.103721.
[102] M. Holloway, J.M. Sykes, Studies of the corrosion of mild steel in alkali-activated slag cement mortars with sodium chloride admixtures by a galvanostatic pulse method, Corros. Sci. 47 (2005) 3097–3110, https://doi.org/10.1016/j.corsci.2005.05.035.
[103] D.W. Shoesmith, P. Taylor, M.G. Bailey, B. Ikeda, Electrochemical behaviour of iron in alkaline sulphide solutions, Electrochim. Acta 23 (1978) 903–916, https://doi.org/10.1016/0013-4686(78)87014-5.
[104] S. Mundra, J.L. Provis, Mechanisms of passivation and chloride-induced corrosion of mild steel in sulfide-containing alkaline solutions, J. Mater. Sci. 56 (2021) 14783–14802, https://doi.org/10.1007/s10853-021-06237-x.
[105] S.M. Abd Haleem, E.E. Abd El Aal, Effect of sulphide ions on corrosion behaviour of iron in alkaline solutions, Corros. Eng. Sci. Technol. 43 (2008) 225–230, https://doi.org/10.1179/174327808×272351.
[106] X. Shen, W. Chen, B. Li, C.M. Hancock, Y. Xu, Flexural strengthening of reinforced concrete beams using fabric reinforced Alkali-Activated Slag matrix, J. Build. Eng. 33 (2021), 101865.
[107] R. Manjunath, M.C. Narasimhan, An experimental investigation on self-compacting alkali activated slag concrete mixes, J. Build. Eng. 17 (2018) 1–12.
[108] S. Aydın, B. Baradan, Sulfate resistance of alkali-activated slag and Portland cement based reactive powder concrete, J. Build. Eng. 43 (2021), 103205.
[109] L.U.D.T. Júnior, M. Taborda-Barraza, M. Cheriaf, P.J.P. Gleize, J.C. Rocha, Effect of bottom ash waste on the rheology and durability of alkali activation pastes, Case Stud. Constr. Mater. 16 (2022), e00790, https://doi.org/10.1016/j.cscm.2021.e00790.
[110] T.H. Vu, N. Gowripalan, P.D. Silva, A. Paradowska, U. Garbe, P. Kidd, V. Sirivivatnanon, Assessing carbonation in one-part fly ash/slag geopolymer mortar: change in pore characteristics using the state-of-the-art technique neutron tomography, Cem. Concr. Compos. 114 (2020), 103759, https://doi.org/10.1016/j.cemconcomp.2020.103759.
[111] B.C. Mendes, L.G. Pedroti, C.M.F. Vieira, M. Marvila, A.R.G. Azevedo, J.M.F. de Carvalho, J.C.L. Ribeiro, Application of eco-friendly alternative activators in alkali-activated materials: a review, J. Build. Eng. 35 (2021), 102010, https://doi.org/10.1016/j.jobe.2020.102010.
[112] L.C. Dang, H. Khabbaz, B.J. Ni, Improving engineering characteristics of expansive soils using industry waste as a sustainable application for reuse of bagasse ash, Transp. Geotech. 100637 (31) (2021) 2214–3912, https://doi.org/10.1016/j.trgeo.2021.100637.
[113] A.R.G. Azevedo, M.T. Marvila, H.A. Rocha, L.R. Cruz, C.M.F. Vieira, Use of glass polishing waste in the development of ecological ceramic roof tiles by the geopolymerization process, Int. J. Appl. Ceram. Technol. 6 (2020) 2649–2658, https://doi.org/10.1111/ijac.13585.